Atmos. Chem. Phys. Discuss., https://doi.org/10.5194/acp-2017-768
Manuscript under review for journal Atmos. Chem. Phys.
Discussion started: 20 September 2017

Atmospheric Chemistry and Physics Discussions

Revising global ozone dry deposition estimates based on a new mechanistic parameterisation for air-sea exchange and the multi-year MACC composition reanalysis

Ashok K. Luhar[1], Matthew T. Woodhouse[1], Ian E. Galbally[1]

[1]CSIRO Oceans and Atmosphere, Aspendale, 3195, Australia

Correspondence to: Ashok K. Luhar (ashok.luhar@csiro.au)

Abstract. Dry deposition at the Earth's surface is an important sink of atmospheric ozone. Currently, dry deposition of ozone to the ocean surface in atmospheric chemistry models has the largest uncertainty compared to deposition to other surface types, with implications for global tropospheric ozone budget and associated radiative forcing. Most models assume that the dominant term of surface resistance in the parameterisation of ozone dry deposition velocity at the oceanic surface is constant. We present a consistent, process-based parameterisation scheme for air-sea exchange in which the surface resistance accounts for the simultaneous waterside processes of ozone solubility, molecular diffusion, turbulent transfer, and a first-order chemical reaction of ozone with dissolved iodide. The new scheme makes the following realistic assumptions: (a) the thickness of the top water layer is of the order of a reaction-diffusion length scale (a few micrometres) within which ozone loss is dominated by chemical reaction and the influence of waterside turbulent transfer is negligible; (b) in the water layer below, both chemical reaction and waterside turbulent transfer act together and are accounted for; and (c) iodide (hence chemical reactivity) is present through the depth of the oceanic mixing layer. The asymptotic behaviour of the new scheme is consistent with the known limits when either chemical reaction or turbulent transfer dominates. It has been incorporated into the ACCESS-UKCA global chemistry-climate model and the results are evaluated against dry deposition velocities from currently best available open-ocean measurements. In order to better quantify the global dry deposition loss and its interannual variability, the modelled 3-h ozone deposition velocities are combined with the 3-h MACC (Monitoring Atmospheric Composition and Climate) reanalysis ozone for the years 2003–2012. The resulting ozone dry deposition is found to be 98.4 ± 4.5 Tg O_3 yr^{-1} for the ocean and 722.8 ± 20.9 Tg O_3 yr^{-1} globally. The new estimate of the ocean component is approximately a third of the current model estimates. This reduction corresponds to an approximately 20% decrease in the total global ozone dry deposition, which is equivalent to an increase of approximately 5% in the modelled tropospheric ozone burden and a similar increase in tropospheric ozone lifetime.

Atmos. Chem. Phys. Discuss., https://doi.org/10.5194/acp-2017-768
Manuscript under review for journal Atmos. Chem. Phys.
Discussion started: 20 September 2017

Atmospheric Chemistry and Physics Discussions

1 Introduction

Ozone (O_3) in the atmosphere acts as a greenhouse gas, and adversely impacts human health and plant productivity (e.g., Young et al., 2013; Monks et al., 2015). In the troposphere, the budget of ozone is determined by its transport from the stratosphere, dry deposition at the Earth's surface, and chemical production and loss. Dry deposition is a significant sink of ozone (Galbally and Roy, 1980), influencing ozone concentration, its lifetime and long range transport. The average dry deposition velocity of O_3 to the ocean is less than that to terrestrial surfaces, but because of the larger coverage of the Earth's surface by the oceans there is substantial dry deposition to water. The 'present-day' (~2000) total global dry deposition of O_3 estimated by climate–chemistry models is reported to be 1094 ± 264 Tg yr^{-1} (IPCC, 2013; Young et al., 2013), of which about 35% is to the ocean (Ganzeveld et al., 2009; Hardacre et al., 2015). Hardacre et al. (2015) observed that ozone dry deposition to the water surface in models has the largest uncertainty compared to other surface types. A proper treatment of dry deposition to the ocean in atmospheric chemistry models is thus necessary for more realistic ozone estimates and better representation of feedback cycles, e.g. that involving iodine chemistry (Carpenter et al., 2013). Although dry deposition of ozone to the ocean is the focus of the present paper, we also place ocean dry deposition in the context of total global dry deposition and examine its interannual variability. In this paper the word deposition means dry deposition.

The dry deposition flux, F_{O_3}, of ozone to the surface is normally calculated as the product of its concentration, $[O_3]$, in the air near the surface and a (downward) dry deposition velocity, v_d:

$$F_{O_3} = v_d . [O_3] . \quad (1)$$

A common approach to parameterising v_d is to express it as a linear sum of three resistances (e.g., Wesely, 1989):

$$v_d = \frac{1}{r_a + r_b + r_c} , \quad (2)$$

where the aerodynamic resistance r_a is the resistance to transfer by turbulent mixing in the atmospheric surface layer, the atmospheric viscous, or quasi laminar, sublayer resistance r_b is the resistance to movement across a thin layer (0.1 – 1 mm) of air that is in direct contact with the surface, and the surface resistance r_c is the resistance to uptake by the surface itself that can be controlled by physical, chemical, biological or other processes depending on the surface type and species of interest.

Atmos. Chem. Phys. Discuss., https://doi.org/10.5194/acp-2017-768
Manuscript under review for journal Atmos. Chem. Phys.
Discussion started: 20 September 2017

Atmospheric Chemistry and Physics Discussions

For ozone dry deposition to water surfaces, r_c is the dominant term in Eq. (2). It is commonly assumed that r_c is constant (≈ 2000 s m^{-1}) based on Wesely's (1989) deposition parameterisation, and this approach is used by default in most global chemical transport models, e.g. MATCH-MPIC (von Kuhlmann et al., 2003), MESSy (Kerkweg et al., 2006), MOZART-4 (Emmons et al., 2010), CAM-chem (Lamarque et al., 2012), GEOS-Chem (Mao et al., 2013) and UKCA (Abraham et al., 2012).

Recently, Luhar et al. (2017) demonstrated that the use of a constant r_c results in an unrealistic, near-constant behaviour of v_d which progressively overestimates the best available, open-ocean deposition velocity measurements (Helmig et al., 2012) by a factor of 2 to 4 as sea surface temperatures (SSTs) decrease.

Luhar et al. (2017) formulated a two-layer reactivity scheme for r_c based on the approach of Fairall et al. (2007) which derives r_c by solving a simplified form of the mass conservation equation for ozone and includes the influence of waterside processes acting on ozone, namely solubility, molecular diffusion, turbulent transfer and a first-order chemical reaction of ozone with dissolved iodide (deposition velocity increases as the magnitude of each of these processes increases).

At this point it is useful to define the waterside layers near the sea surface that are relevant here. The top few millimetres of the sea surface is often termed the sea surface microlayer which may be composed of various sublayers or scales depending on the physical, chemical or biological properties being considered (Soloviev and Lukas, 2014; Carpenter et al., 2015). Very close to the water surface is a viscous sublayer (~ 1 mm) within which viscous processes dissipate the turbulent kinetic energy associated with the smallest of the eddies (of the size of Kolmogorov microscale) into heat. Thus the viscous sublayer thickness is of the order of the level at which the turbulent eddy diffusivity falls below the kinematic viscosity. A level exists within the viscous sublayer at which the diminishing eddy diffusivity falls below the molecular diffusivity, and this level is approximately the thickness of the diffusive sublayer (~ 50 μm for ozone). Embedded within the diffusive sublayer can be another sublayer (which we call reaction-diffusion sublayer) characterised by chemical reactivity and molecular diffusivity, whose thickness is scaled by a reaction-diffusion length scale (typically 3 μm for the ozone-iodide reaction in water). In the surface turbulent layer (~ 10–50 m) below the surface microlayer, turbulent processes dominate.

In the Luhar et al. (2017) formulation, the chemical reactivity of ozone with dissolved iodide within the reaction-diffusion sublayer (δ_m ~ 3 μm) was determined as the product of the pertinent second-order rate coefficient and iodide concentration, but in the water region below δ_m it was assumed that there is a near-zero background chemical reactivity, meaning that the iodide concentration below δ_m is virtually zero. The Luhar et al. (2017) scheme when used in a global chemistry-climate model, namely ACCESS-UKCA (Australian Community Climate and Earth System Simulator – United Kingdom Chemistry and Aerosol), was able to describe well the absolute magnitude and the sea surface temperature dependence of the deposition velocity measurements of Helmig et al. (2012) over the ocean.

Atmos. Chem. Phys. Discuss., https://doi.org/10.5194/acp-2017-768
Manuscript under review for journal Atmos. Chem. Phys.
Discussion started: 20 September 2017

Atmospheric Chemistry and Physics Discussions

Although the two-layer reactivity scheme of Luhar et al. (2017) was successful in describing the observations, limiting the chemical reactivity and hence the iodide concentration in this scheme to within a depth of water that is of the order of only a few micrometres is not a realistic assumption because in reality iodide is present through the depth of the oceanic surface turbulent layer (~ 10–50 m) and even deeper (Chance et al., 2014). The primary reason the two-layer reactivity scheme worked well was that limiting the dissolved iodide concentration to the reaction-diffusion sublayer artificially compensated for the effects of the overestimation of turbulent (or eddy) diffusivity (K_t) (see below), thereby effectively restricting the vertical extent of the ozone-iodide reaction and its interaction with turbulence to the thickness of the reaction-diffusion sublayer and circumventing an overestimation of v_d .

The overestimation of K_t alluded to above results from the use of the linear parameterisation $K_t = \kappa u_{*_w} z$ (assuming neutral stratification), where u_{*_w} is the waterside friction velocity, κ is the von Karman constant (= 0.4) and z is depth from the surface. This parameterisation is valid for a fully turbulent surface layer that lies beyond the viscous sublayer. For depths within the viscous sublayer, the viscous dissipation of turbulence causes the eddy diffusivity to diminish much more rapidly with decreasing z than provided by the linear relationship. A more appropriate parameterisation for K_t which varies as z^m in the viscous sublayer where $m = 2–3$ (Fairall et al., 2000) can be considered but a corresponding analytical solution for r_c that includes chemical reaction, molecular diffusion and turbulent transfer has not so far been found.

The aims of the present paper are twofold. First, to formulate an alternative two-layer reaction-diffusion-turbulence parameterisation for r_c that eliminates some of the inconsistencies inherent in the two-layer reactivity scheme reported by Luhar et al. (2017). In particular, the new scheme does not unrealistically limit the iodide concentration to a very thin water layer—instead it makes the valid assumption that iodide is present through the depth of the oceanic mixing layer, which is supported by observations. The new scheme employs a plausible assumption with regards to the extent of reaction-dominated deposition regime, and has an asymptotic behaviour that is consistent with the known limits when turbulent transfer dominates over chemical reaction and vice versa. This new scheme is incorporated into ACCESS-UKCA and the results on deposition velocity are compared with the data of Helmig et al. (2012) and the two-layer reactivity scheme of Luhar et al. (2017).

Second, the oceanic and global dry deposition budgets of ozone are better estimated by combining the global MACC (Monitoring Atmospheric Composition and Climate) reanalysis for ozone concentration fields for ten years (2003–2012) and the ozone deposition velocities estimated from the new scheme. The interannual variability of these budgets is investigated and they are compared with those from other studies.

Atmos. Chem. Phys. Discuss., https://doi.org/10.5194/acp-2017-768
Manuscript under review for journal Atmos. Chem. Phys.
Discussion started: 20 September 2017

Atmospheric Chemistry and Physics Discussions

2 A consistent two-layer scheme for surface resistance r_c

Assuming horizontal homogeneity and stationarity, the mass conservation equation for a chemical species in water is (Geernaert et al., 1998; Fairall et al., 2007):

$$\frac{\partial}{\partial z}\left[\{D+K_t(z)\}\frac{\partial C(z)}{\partial z}\right]-a\,C(z)=0\,, \tag{3}$$

where z is the depth from water surface, $C(z)$ is the concentration of the species, D is the molecular diffusivity of the species in water, $K_t(z)$ is the turbulent diffusivity and a is a first-order reaction rate coefficient (s^{-1}) which for the ozone-iodide reaction ($O_3 + I^- \rightarrow$ products) is determined as the pertinent second-order rate coefficient (k) multiplied by the iodide concentration ($[I^-]$).

A flux variable F_0 (which we will just refer to as flux) that is invariant with water depth z can be defined by integrating Eq. (3) (Fairall et al., 2007):

$$-[D+K_t(z)]\frac{\partial C(z)}{\partial z}+a\int_0^z C(z)dz=F_0\,. \tag{4}$$

The first term on the left hand side of Eq. (4) is the mixing flux (molecular diffusion plus turbulent mixing) which decreases with depth as the reacting gas is absorbed. This component is balanced by the second term on the left hand side which is the integrated loss rate of ozone by chemical reaction between the ocean surface and depth z.

We consider a two-layer approach in which chemical reaction in the top water layer of depth δ_m (i.e. the reaction-diffusion sublayer) is fast enough such that it dominates over turbulent transfer, with the assumption $K_t = 0$, and transport is maintained by molecular diffusion. The thickness of this layer is thus of the order of the so-called reaction-diffusion length scale $l_m = (D/a)^{1/2}$ for the ozone-iodide reaction in seawater which is typically a few micrometres. This length scale for the said reaction is even smaller than the Kolmogorov microscale (the latter is indicative of the smallest of the turbulent eddies present in the flow) so it is fair to assume that $K_t = 0$ within the reaction-diffusion sublayer. The second layer deeper than the reaction-diffusion sublayer (i.e. $z > \delta_m$) has both chemical reaction and turbulent mixing included and a linear parameterisation for turbulent diffusivity $K_t = \kappa u_{*w} z$ is used. The second layer can thus include the viscous sublayer and extend to the surface turbulent layer. The chemical reaction of ozone predominantly occurs in the first layer. In

Atmos. Chem. Phys. Discuss., https://doi.org/10.5194/acp-2017-768
Manuscript under review for journal Atmos. Chem. Phys.
Discussion started: 20 September 2017

Atmospheric Chemistry and Physics Discussions

the second layer, turbulence-chemistry interaction is weak compared to transfer by turbulent mixing. It is therefore reasonable to use a linearly varying K_t throughout the second layer. Both layers have the same reactivity *a*, i.e. the iodide concentration is uniform through the oceanic surface mixed layer. With the above assumptions, Eq. (3) can be solved for concentration in the first (or top) layer (C_1) and that in the second (or bottom) layer (C_2) to yield:

$$C_1(z) = A_1 \exp\left(z\sqrt{\frac{a}{D}}\right) + B_1 \exp\left(-z\sqrt{\frac{a}{D}}\right), \quad (5)$$

$$C_2(z) = B_2 K_0(\xi), \quad (6)$$

where $\xi = [2ab(z + (bD/2))]^{1/2}$, $b = 2/(\kappa u_{*_w})$, κ= 0.4, and $K_0(\xi)$ is the modified Bessel function of the second kind of order 0.

The expressions for the mixing component (which includes both turbulent and molecular diffusion parts) of flux F_0 in the first and second layers follow from the first part on the left hand side of Eq. (4) coupled with Eqs. (5) and (6):

$$F_{m1}(z) = -(aD)^{1/2}\left[A_1 \exp\left(z\sqrt{\frac{a}{D}}\right) - B_1 \exp\left(-z\sqrt{\frac{a}{D}}\right)\right], \quad (7)$$

$$F_{m2}(z) = \frac{B_2}{b}\xi K_1(\xi), \quad (8)$$

where and $K_1(\xi)$ is the modified Bessel function of the second kind of order 1.

The three unknown coefficients A_1, B_1 and B_2 are determined by imposing three boundary conditions. The first two, namely the flux at the water surface ($z = 0$) obtained using Eq. (4) should be equal F_0 and the concentration at the interface of the two layers ($z = \delta_m$) should be continuous, lead to the following equations, respectively:

$$F_0 = F_{m1(z=0)} = (a\,D)^{1/2}(-A_1 + B_1), \quad (9)$$

$$A_1 \exp(\lambda) + B_1 \exp(-\lambda) - B_2 K_0(\xi_\delta) = 0, \quad (10)$$

where $\xi_\delta = [2ab(\delta_m + (bD/2))]^{1/2}$ and $\lambda = \delta_m(a/D)^{1/2}$.

The third boundary condition can be imposed in a couple of ways, both of which lead to the same answer. First, the total flux at the interface is continuous, i.e.

Atmos. Chem. Phys. Discuss., https://doi.org/10.5194/acp-2017-768
Manuscript under review for journal Atmos. Chem. Phys.
Discussion started: 20 September 2017

Atmospheric Chemistry and Physics Discussions

$$F_{m1}(\delta_m) + a\int_0^{\delta_m} C_1(z)dz = F_{m2}(\delta_m) + a\int_0^{\delta_m} C_1(z)dz\,, \tag{11}$$

which leads to $F_{m1}(\delta_m) = F_{m2}(\delta_m)$. This after substituting the flux Equations (7) and (8) yields

$$(aD)^{1/2}\{A_1\exp(\lambda) - B_1\exp(-\lambda)\} + \frac{B_2}{b}\xi_\delta K_1(\xi_\delta) = 0\,. \tag{12}$$

Another option as used by Fairall et al. (2007) is that as $z \to \infty$ the mixing term in Eq. (4) becomes 0 so F_0 equals the total absorption of concentration by chemical reaction, i.e.

$$F_0 = a\int_0^{\delta_m} C_1(z)dz + a\int_{\delta_m}^{\infty} C_2(z)dz\,. \tag{13}$$

This condition leads to exactly the same expression as Eq. (12) when F_0 is substituted from Eq. (9).

Solving Eqs. (9), (10) and (12) yields

$$B_1 = \frac{F_0\exp(\lambda)}{2(aD)^{1/2}}\left[\frac{\psi K_1(\xi_\delta) + K_0(\xi_\delta)}{\psi K_1(\xi_\delta)\cosh(\lambda) + K_0(\xi_\delta)\sinh(\lambda)}\right]. \tag{14}$$

Now A_1 and B_2 can be determined using Eq. (9) and (10), respectively, after substituting B_1 from Eq. (14). Using Eqs. (5) and (9) we can obtain an expression for the waterside deposition velocity v_{dw} as the flux (F_0) divided by concentration (C_0) at $z = 0$

$$v_{dw} = (aD)^{1/2}\left[\frac{-A_1 + B_1}{A_1 + B_1}\right], \tag{15}$$

which after substituting for A_1 and B_1 yields

$$v_{dw} = (aD)^{1/2}\left[\frac{\psi K_1(\xi_\delta)\cosh(\lambda) + K_0(\xi_\delta)\sinh(\lambda)}{\psi K_1(\xi_\delta)\sinh(\lambda) + K_0(\xi_\delta)\cosh(\lambda)}\right], \tag{16}$$

Atmos. Chem. Phys. Discuss., https://doi.org/10.5194/acp-2017-768
Manuscript under review for journal Atmos. Chem. Phys.
Discussion started: 20 September 2017

Atmospheric Chemistry and Physics Discussions

where $\psi = \xi_\delta / (a\,b^2 D)^{1/2} = [1 + (\kappa u_{*w} \delta_m / D)]^{1/2}$. Eq. (16) is the final expression for v_{dw} and is used to determine r_c as

$$r_c = \frac{1}{\alpha v_{dw}}, \tag{17}$$

where α is the dimensionless solubility of ozone in water (which is the ratio of the aqueous-phase ozone concentration to its gas-phase concentration and is related to Henry's law coefficient).

2.1 Asymptotic limits

In the limit $\delta_m \to 0$, Eq. (16) reduces to

$$v_{dw} = (a\,D)^{1/2} \left[\frac{K_1(\xi_0)}{K_0(\xi_0)} \right], \tag{18}$$

where $\xi_0 = b(a\,D)^{1/2}$. This is equivalent to the one-layer model of Fairall et al. (2007) which employs a linearly varying K_t with z and which overestimates the oceanic deposition velocity measurements of Helmig et al. (2012) by a factor of 2–3 (Luhar et al., 2017).

In the limit $\delta_m \to \infty$, the waterside turbulent transfer is neglected and the formulation becomes equivalent to the diffusion-reaction formulation considered by Garland et al. (1980):

$$v_{dw} = (a\,D)^{1/2}, \tag{19}$$

which underestimates the oceanic deposition velocity measurements of Helmig et al. (2012) for SSTs below 15°C (Luhar et al., 2017).

2.2 Behaviour of the new scheme and specification of δ_m

The above scheme requires specification of the dissolved iodide concentration $[I^-]$, the second-order rate coefficient (k) for the ozone-iodide reaction used in the calculation of chemical reactivity via $a = k.[I^-]$, the dimensionless solubility of ozone in water (α), and the molecular diffusivity of ozone in water (D). In the first case the parameterisations employed by Luhar et al. (2017) are used.

Atmos. Chem. Phys. Discuss., https://doi.org/10.5194/acp-2017-768
Manuscript under review for journal Atmos. Chem. Phys.
Discussion started: 20 September 2017

Atmospheric Chemistry and Physics Discussions

$$[I^-] = 1.46\times10^6 \exp\left(\frac{-9134}{T_s}\right) \quad (20)$$

from MacDonald et al. (2014) where $[I^-]$ is in mole per litre (or molar, M) and T_s (K) is the water temperature.

The quantity k (M^{-1} s^{-1}) based on the data from Magi et al. (1997) is

$$k = \exp\left(\frac{-p}{T_s} + q\right), \quad (21)$$

where $p = 8772.2$ and $q = 51.5$.

The solubility is (Morris, 1988)

$$\log_{10}(\alpha) = -0.25 - 0.013(T_s - 273.16). \quad (22)$$

The quantity D (m^2 s^{-1}) is given as (Johnson and Davis, 1996)

$$D = 1.1\times10^{-6} \exp\left(\frac{-1896}{T_s}\right). \quad (23)$$

The waterside friction velocity u_{*w} is calculated as $u_{*w} = (\rho_a/\rho_w)^{1/2} u_*$ where u_* is the airside friction velocity, ρ_a is the air density and ρ_w is the water density.

The depth δ_m needs to be specified. As mentioned earlier, it is of the order of the reaction-diffusion length scale $l_m [= (D/a)^{1/2}]$ so one option is to take $\delta_m = c_0 l_m$ where c_0 is a constant (in that case $\lambda = c_0$ is constant). (With the above parameterisations for $[I^-]$, k and D, l_m varies between 24.0–1.2 μm for the SST range 2–33°C, and it is 3 μm at 23°C.) Figure 1 presents the variation of the oceanic component of dry deposition velocity multiplied by the ozone solubility, i.e. αv_{dw} (=$1/r_c$), calculated from Eq. (16) as a function of SST (Figure 1a) and reactivity (a) (Figure 1b) for three c_0 values for a typical value of the waterside friction velocity (u_{*w}) of 0.01 m s^{-1} (which corresponds to an airside u_* of approximately 0.3 m s^{-1}). The plotted variations show that αv_{dw} increases with SST and with the logarithm of a in a very similar manner. As c_0 decreases (hence δ_m decreases) the two-layer model behaviour approaches the behaviour of the one-layer scheme given by Eq. (18) in which turbulent diffusivity is a linear function of depth and chemical reaction is included.

Atmos. Chem. Phys. Discuss., https://doi.org/10.5194/acp-2017-768
Manuscript under review for journal Atmos. Chem. Phys.
Discussion started: 20 September 2017

Atmospheric Chemistry and Physics Discussions

On the other hand, as c_0 gets larger (hence δ_m gets larger) the extent of the reaction-diffusion regime in the two-layer scheme gets larger and the model behaviour approaches the limiting behaviour $\alpha v_{dw} = \alpha(a\,D)^{1/2}$ (Eq. (19)) as originally discussed by Garland et al. (1980). In the two-layer reactivity scheme of Luhar et al. (2017), in some cases αv_{dw} can go below the variation implied by the diffusion-reaction limit (19) which is not realistic and which does not occur in the new scheme.

In Figure 1b, as *a* decreases δ_m increases (since $\delta_m = c_0 (D/a)^{1/2}$) the model approaches the diffusion-reaction limit Eq. (19) of Garland et al. (1980), and as *a* increases δ_m decreases and the model approaches the one-layer solution Eq. (18). Figure 1a shows the same behaviour but in terms of SST.

Another method for specifying δ_m is to assume that it is constant. Figure 1 shows the variation of αv_{dw} calculated from Eq. (16) as a function of SST (Figure 1c) and *a* (Figure 1d) for several fixed values of δ_m between 0.5 and 10 μm. These variations look different compared to those in Figure 1a and Figure 1b but like the latter they all fall within the two limits. As δ_m decreases the αv_{dw} variation approaches the one-layer solution Eq. (18) and as δ_m increases this variation approaches the diffusion-reaction limit Eq. (19).

It is found that the use of $\delta_m = c_0\, l_m$ (so $\lambda = c_0$) together with the parameterisations (20)–(23) does not fullydescribe the variation of the measured deposition velocities with SST (presented later) regardless of the value of c_0. For example, with $c_0 = 0.7$ there is an underestimation by the model of the measured deposition velocities for SSTs less than 18°C and an overestimation for higher SSTs. For $c_0 < 0.7$ the overestimation gets worse. For $c_0 > 0.7$ the underestimation gets worse and the αv_{dw} variation approaches the diffusion-reaction behaviour.

Atmos. Chem. Phys. Discuss., https://doi.org/10.5194/acp-2017-768
Manuscript under review for journal Atmos. Chem. Phys.
Discussion started: 20 September 2017

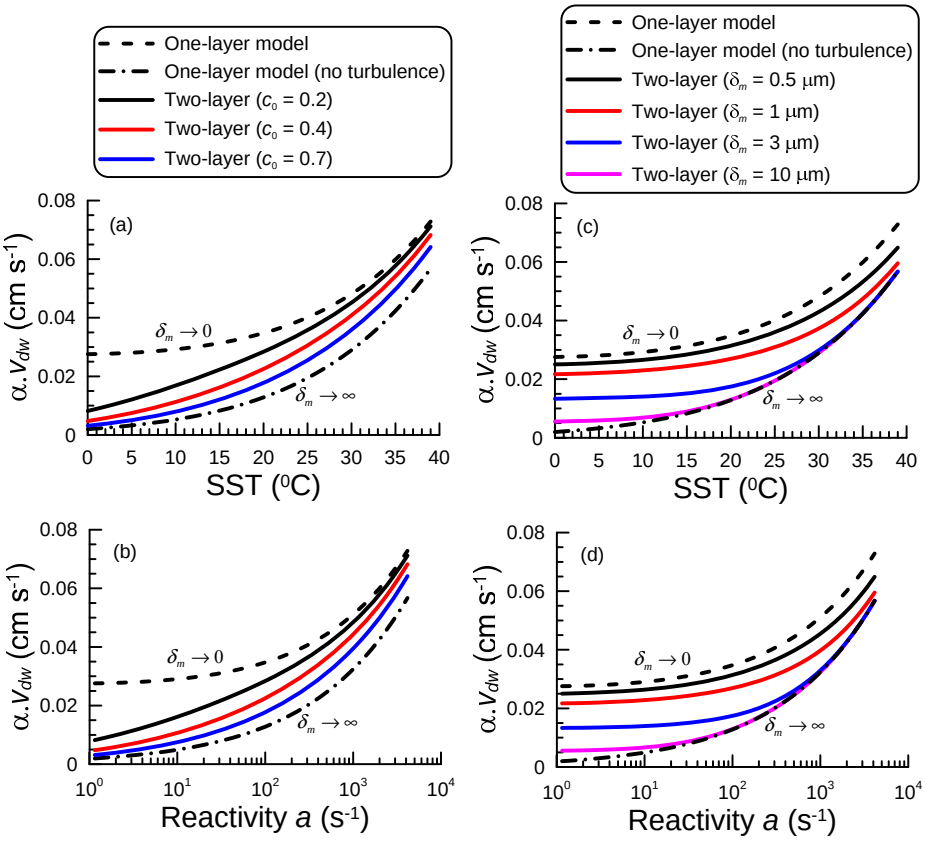

Figure 1: Variation of the oceanic component of ozone dry deposition velocity multiplied by ozone solubility, αv_{dw} (= $1/r_c$), as a function of (a, c) sea surface temperature (SST, °C) and (b, d) reactivity *a* (s^{-1}). Curves determined using the two-layer deposition scheme (Eq. (16)) for (a, b) several c_0 values used in $\delta_m = c_0 l_m$ and (c, d) several δ_m values. The variations obtained using the one-layer deposition scheme with (Eq. (18)) and without (Eq. (19)) waterside turbulent transfer (i.e. reaction-diffusion only) are also shown. The waterside friction velocity (u_{*w}) used was 0.01 m s^{-1}.

There are further considerations to the parameterisations. There is uncertainty in the parameterisations (20)–(23), particularly in the second-order rate coefficient *k* for which there is a paucity of data. The expression (21) is based on the data from Magi et al. (1997) which are plotted in Figure 2 with the associated uncertainty. Also, plotted are the single data points from Garland et al. (1980), Hu et al. (1995) and Liu et al. (2001). Clearly there is a large scatter in the data. Five cases are

Atmos. Chem. Phys. Discuss., https://doi.org/10.5194/acp-2017-768
Manuscript under review for journal Atmos. Chem. Phys.
Discussion started: 20 September 2017

Atmospheric Chemistry and Physics Discussions

considered with regards to parameterising *k* via an exponential fit of the form Eq. (21): 1) only consider the data of Magi et al. (1997) (so the fit is the same as Eq. (21) with stated *p* and *q* values); 2) consider all the data (which gives $p = 2349.2$ and $q = 29.2$); 3) consider all the data except the data point of Hu et al. (1995) which is treated as an outlier (which gives $p = 5632.9$ and $q = 40.3$); 4) assume a constant $\delta_m = 3\,\mu m$ with *k* given by Eq. (21) using only the data of Magi et al. (1997); and 5) assume a constant $k = 2\times10^9$ $M^{-1}\,s^{-1}$ as in MacDonald et al. (2014). We used $c_0 = 0.4$ in calculating $\delta_m = c_0\, l_m$ in all the above options, except option (4) which does not need c_0. Figure 3 shows the variation of αv_{dw} calculated from Eq. (16) as a function of SST for the above five options. All five options provide qualitatively similar variations of αv_{dw}, but when compared with the cruise measurements of oceanic deposition velocities discussed later (which themselves have substantial scatter), options (3) and (4) provide better agreement overall with the measurements compared to the other options. Option (3) tends to underestimate the observed deposition velocities by roughly 15% for SSTs less than around 12°C whereas option (4) tends to overestimate them by about the same degree. For higher SSTs, both options perform similarly, with option (4) being very slightly better for SSTs greater than 20°C, within the scatter of the measurements. In all the calculations below we have used option (4) for δ_m and *k* in ACCESS-UKCA.

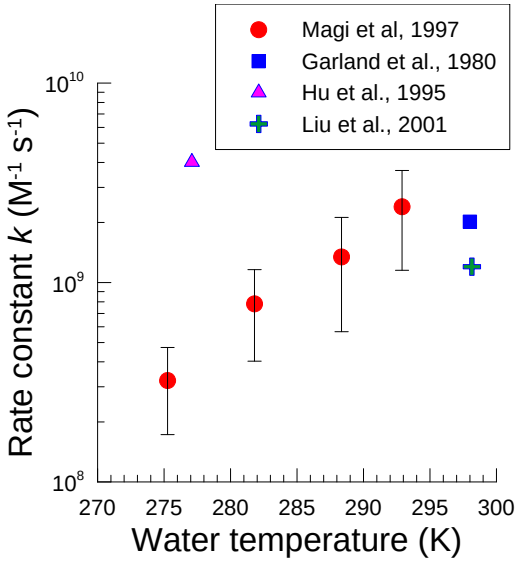

Figure 2: The second-order rate coefficient (*k*) for the ozone-iodide reaction as a function of water temperature. Data from various studies are shown.

Atmos. Chem. Phys. Discuss., https://doi.org/10.5194/acp-2017-768
Manuscript under review for journal Atmos. Chem. Phys.
Discussion started: 20 September 2017

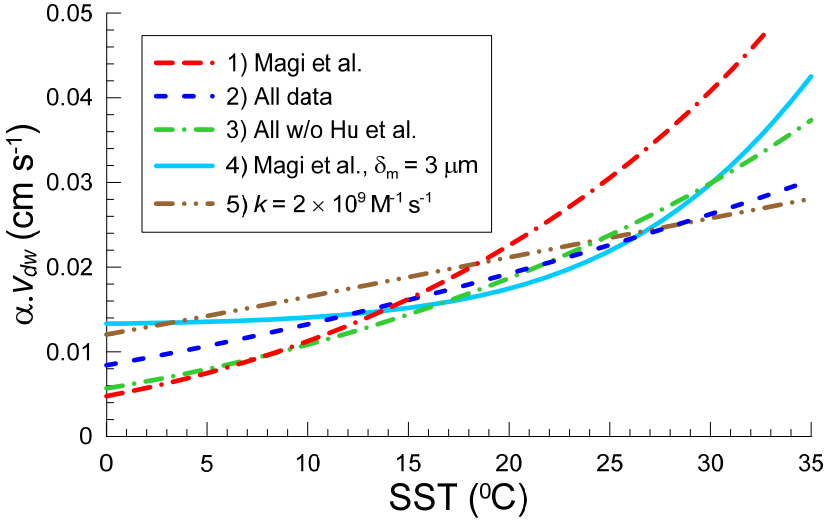

Figure 3: Variation of the oceanic component of ozone dry deposition velocity multiplied by ozone solubility, αv_{dw} (= $1/r_c$), as a function of sea surface temperature (SST, °C). Curves determined using the two-layer deposition scheme (Eq. (16)) for various options for parameterising the second-order rate coefficient (*k*) (see text). The waterside friction velocity (u_{*w}) used was 0.01 m s^{-1}.

3 ACCESS-UKCA chemistry-climate modelling system

The two-layer dry deposition scheme developed above was incorporated into the UK Chemistry and Aerosol (UKCA, http://www.ukca.ac.uk) global atmospheric composition model (at UM vn8.4; see Morgenstern et al., 2009; Abraham et al., 2012; O'Connor, 2014) which is a component in the Australian Community Climate and Earth System Simulator (ACCESS, Woodhouse et al., 2015). The physical atmosphere component of ACCESS is the UK Met Office's Unified Model (MetUM), and the joint model is referred to here as ACCESS-UKCA. The particular UKCA configuration used here (at UM vn8.4) is the so-called Chemistry of the Stratosphere and Troposphere (CheST), which includes O_x, HO_x, NO_x and volatile organic carbon chemistry in addition to bromine and chlorine chemistry relevant for stratospheric ozone. ACCESS-UKCA uses an atmosphere-only configuration with monthly-mean sea surface temperature and sea ice fields prescribed from the Atmospheric Model Intercomparison project (AMIP). The atmospheric model has a horizontal resolution of 1.875° in

longitude and 1.25° in latitude, and 85 levels extending from the surface to approximately 85 km (the N96L85 configuration). The model was nudged to the ERA-Interim reanalyses (Dee et al., 2011), given on pressure levels, for the horizontal wind and potential temperature in the free troposphere (Uhe and Thatcher, 2015). Other model setup details including monthly-varying emissions are as in Woodhouse et al. (2015), except that the GFED4s (http://www.globalfiredata.org; van der Werf et al., 2017) rather than the ACCMIP (Atmospheric Chemistry and Climate Model Intercomparison Project) biomass burning emissions were used in the present study to incorporate interannual variability of these emissions. There are nine surface types in the model, namely broad-leaf trees, needle-leaf trees, C3 grass, C4 grass, shrub, urban, water, bare soil, and land ice. For any particular surface grid box the three resistances r_a, r_b and r_c are calculated for each surface type and a corresponding v_d is then computed. For the water surface, standard expressions for r_a and r_b are used by ACCESS-UKCA in Eq. (2) (see Abraham et al., 2012; Luhar et al., 2017) and r_c is computed using Eq. (17) together with the new expression (16). A grid-box mean deposition loss rate is then calculated using the individual deposition velocities weighted by the fractions of the surface types present in the grid box and this loss rate is applied to the lowest model grid box in the species mass conservation equation.

4 Ozone dry deposition velocity to the ocean

4.1 Comparison with observations

We use the ozone dry deposition velocity measurements of Helmig et al. (2012) taken over the open ocean from a ship-based eddy-covariance ozone flux system during 2006–2008 which spanned 45°N to 50°S. The experiments were conducted on five cruises, namely: (1) TexAQS06 (July 7 to September 12, 2006), (2) STRATUS06 (October 9–27, 2006), (3) GOMECC07 (July 11 to August 4, 2007), (4) GasEx08 (February 29 to April 11, 2008), and (5) AMMA08 cruises (April 27 to May 18, 2008). The respective areas covered were: (1) North-western Gulf of Mexico, (2) the persistent stratus cloud region off Chile in the eastern Pacific Ocean, (3) the Gulf of Mexico and the US east coast, (4) the Southern Ocean, and (5) the southern and northern Atlantic Ocean. Helmig et al. (2012) present bin-averaged deposition velocity data as a function of SST and wind speed for each of the five cruises. As in Luhar et al. (2017), the v_d versus SST cruise data used for comparison with the model are those with the wind speed dependence retained (Ludovic Bariteau, personal communication, 2016) and not the data originally reported by Helmig et al. (2012) in which the wind-speed dependence was removed. While this approach is logically correct, there is not a large difference between the data with and without the wind-speed dependence.

ACCESS-UKCA output including dry deposition parameters is available at 3-h time intervals and also as monthly averages over the period 2003–2012, which covers the time period of the Helmig et al. (2012) observations. Because the data are averaged with respect to SST or wind-speed bins for each cruise and as a result there is no explicit dependence present as to the exact timings and locations of the data along a cruise track, we used the same methodology as that in Luhar et al. (2017)

for comparing the v_d data with ACCESS-UKCA. In summary, as the months corresponding to the cruise experiments are known, the model monthly averages matching the experimental months were selected. For a given month, the monthly-averaged model output was extracted at a series of grid-point locations with almost uniform spacing along the tracks of the experimental cruises, and the modelled values at these points were used for comparison with the measurements. This is an approximate matching of the deposition velocity data and the modelled values in terms of time and location.

Figure 4 shows the observed ozone dry deposition velocity (v_d) as a function of SST from the five field experiments and the corresponding values obtained from the ACCESS-UKCA model using the new two-layer scheme (Eq. (16)). The SST range for the measurements is 2–33 °C with the lowest values being for GasEx08 and the highest for TexAQS06 and GOMECC07. Despite the large fluctuations within the field data, an increasing trend of v_d with SST is clearly noticeable. Helmig et al. (2012) compiled a historical record of ozone deposition velocities over water (their Figure 4) starting from 1969 which lie within the range 0.01–0.15 cm s^{-1}. The range of the cruise measurements in Figure 4, which are the only direct, open-ocean flux measurements, is 0.005 – 0.06 cm s^{-1} which is on the lower end of the range of the historical data. As stated by Helmig et al. (2012), the earlier experiments, lacking ocean-deployable measurement techniques, are biased toward coastal waters which may carry higher concentrations of ozone reactants that lead to increased deposition velocities. Another reason for the difference could be the use of improved experimental techniques in the cruise measurements.

In Figure 4, ACCESS-UKCA is able to describe the absolute magnitude and the sea surface temperature dependence of the field measurements, with the modelled variation almost passing through the middle of the data. However, it is clear that there are some significant fluctuations in the measurements, particularly for SSTs within the range 8–24 °C, that are not present as prominently in the modelled values. There could be a number of possible reasons for this: 1) the monthly-averaged modelled deposition values used and the approximate method followed for matching the data and for time and location; 2) the dissolved iodide concentrations are not directly available and the parameterisation used here only depends on SST; and 3) the observed SSTs used in our atmosphere-only model set up are monthly averaged—a model setup with a coupled ocean model that interacts with the atmosphere at sub-diurnal intervals would provide a better SST variability which would in turn influence the variability in the iodide concentration and thus impact the modelled deposition velocity. Needless to say, additional measurements of ozone dry deposition velocity and governing parameters (e.g. iodide concentrations) with greater temporal and spatial coverage would help to further assess the scheme.

Overall, the model results in Figure 4 are very similar to those obtained by Luhar et al. (2017) using their two-layer reactivity scheme (their Figure 6), and this is evident from the scatter-plot comparison in Figure 5. Figure 5 also shows that for $v_d > 0.022$ cm s^{-1}, the new-scheme values are lower, typically by 5%, and for v_d greater than this value the new-scheme values are greater, typically by 15%. As shown earlier, these differences are sensitive to how δ_m is parameterised.

Atmos. Chem. Phys. Discuss., https://doi.org/10.5194/acp-2017-768
Manuscript under review for journal Atmos. Chem. Phys.
Discussion started: 20 September 2017

Atmospheric Chemistry and Physics Discussions

The model performance presented in Figure 4 leads us to conclude that new scheme performs as well as the two-layer reactivity scheme in Luhar et al. (2017) but unlike the latter the new scheme does not unrealistically/artificially limit the chemical reactivity to within a fixed depth of the order of a few micrometres and has consistent asymptotic limits.

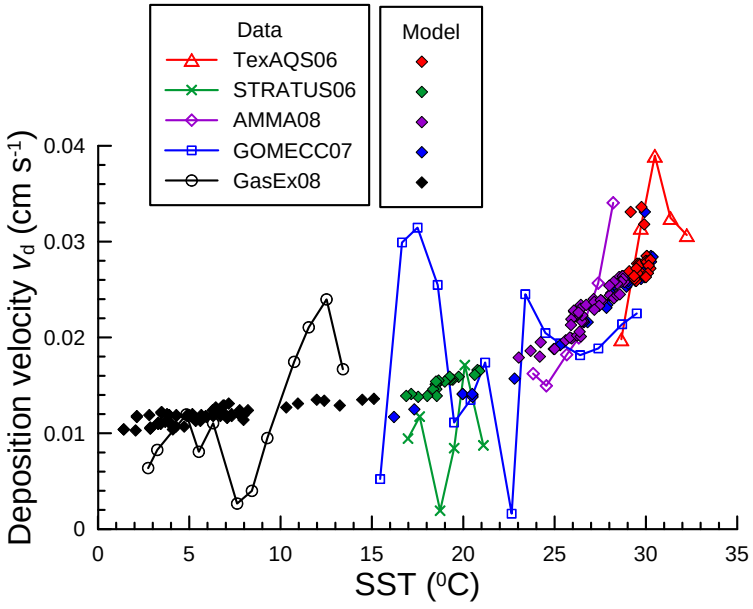

Figure 4: Ozone dry deposition velocity (v_d) as a function of sea surface temperature (SST) from five field experiments (Helmig et al., 2012; Ludovic Bariteau, personal communication, 2016) and the corresponding values obtained from the ACCESS-UKCA model using the new two-layer scheme (Eq. (16)) for ozone deposition to the ocean.

Atmos. Chem. Phys. Discuss., https://doi.org/10.5194/acp-2017-768
Manuscript under review for journal Atmos. Chem. Phys.
Discussion started: 20 September 2017

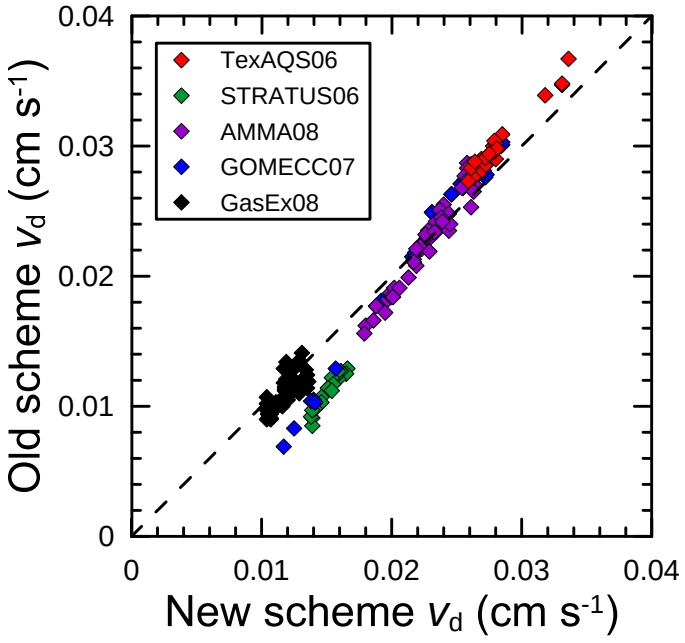

Figure 5: Comparison of the ozone dry deposition velocities (v_d) for the five field experiments obtained from the ACCESS-UKCA model using the new two-layer scheme (Eq. (16)) presented in this paper and those using the old two-layer reactivity scheme of Luhar et al. (2017).

4.2 Global distribution

Figure 6 shows the distribution of ozone deposition velocity (cm s^{-1}) to the ocean obtained using ACCESS-UKCA for the year 2005. The year 2005 is chosen to illustrate the spatial variability because, as will be discussed later, the MACC ozone reanalysis has the least bias for this year (however, we note that the interannual variability of the modelled deposition velocity fields is small). The largest deposition velocities occur in the tropics where both the observed (Chance et al., 2014; MacDonald et al., 2014) and parameterised iodide concentrations, which are proportional to SST, are the largest, and the magnitude of deposition velocities decreases with increasing latitude.

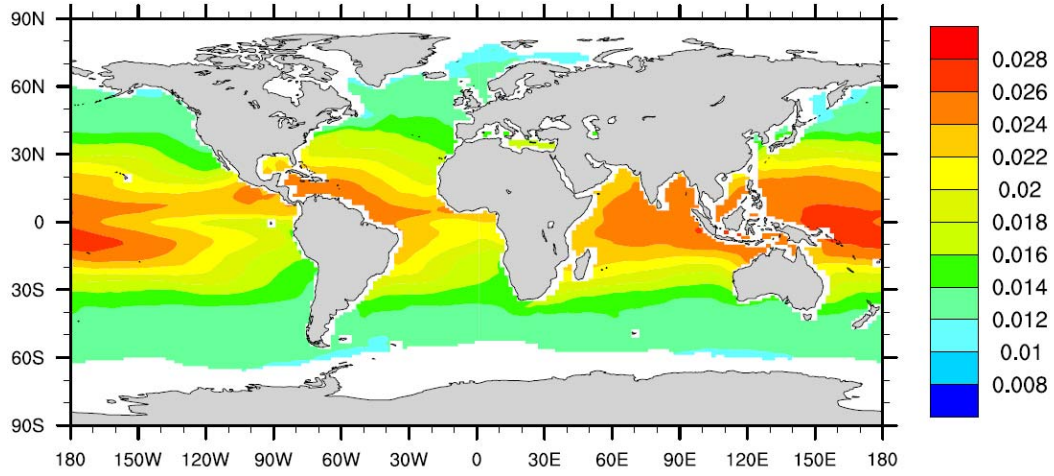

Figure 6: Annual mean ozone dry deposition velocity (v_d, cm s^{-1}) to the ocean for the year 2005 obtained from the ACCESS-UKCA model incorporating with the oceanic dry deposition scheme proposed in this paper.

The multi-annual global mean ozone dry deposition obtained using ACCESS-UKCA for the years 2003–2012 is 86.1 ± 0.9 Tg O_3 yr^{-1} to the ocean and 566.7 ± 4.9 Tg O_3 yr^{-1} globally, where the uncertainty corresponds to one standard deviation and is due to interannual variation. (In our calculations, the water surface excludes sea ice and coastal grid cells and on average covers 62.4% of the Earth's surface.) It is recognised (Woodhouse et al., 2015; Luhar et al., 2017) that ACCESS-UKCA generally underestimates observed tropospheric ozone and that would lead to smaller dry deposition flux given that the deposition velocity is not influenced by the modelled ozone concentration. Luhar et al. (2017) found that improving parameterisation of ozone dry deposition to the ocean reduced the underestimation in the modelled tropospheric ozone compared to measurements but not to the extent whereby it could explain the model-data difference adequately.

Dry deposition velocities were calculated using ACCESS-UKCA at 3-hourly internals and at every grid point for the years 2003–2012. These dry deposition velocities can be used to calculate deposition flux (and hence the annual deposition loss) by using another, more reliable source of near-surface ozone data, given that the deposition flux is the product of the deposition velocity and ozone concentration near the surface. Below, we follow this approach and use a high-resolution global reanalysis of atmospheric ozone data for the period 2003–2012 that is available as part of the Monitoring Atmospheric Composition and Climate (MACC) project (Inness et al., 2013; http://apps.ecmwf.int/datasets/data/macc-reanalysis).

Atmos. Chem. Phys. Discuss., https://doi.org/10.5194/acp-2017-768
Manuscript under review for journal Atmos. Chem. Phys.
Discussion started: 20 September 2017

5 Dry deposition budgets using the MACC ozone reanalysis

The global model used for MACC reanalysis consists of the European Centre for Medium-Range Weather Forecasts' (ECMWF) Integrated Forecast System (IFS) coupled to the MOZART (Model for OZone And Related chemical Tracers) chemistry transport model (Kinnison et al., 2007). The modelling system makes use of four-dimensional variational data assimilation to combine satellite retrievals of carbon monoxide, ozone, nitrogen oxides as well as the standard meteorological observations with the numerical model in order to produce a reanalysis of atmospheric composition. For ozone, profile, total column and partial column data are assimilated.

The MACC reanalysis has been evaluated against multiple observational networks of ground-based measurements, ozonesondes, and aircraft and satellite data (Inness et al., 2013; Gaudel et al., 2015; Giordano et al., 2015; Katragkou et al., 2015; http://macc.copernicus-atmosphere.eu/documents/maccii/deliverables/val/MACCII_VAL_DEL_D_83.6_REAreport04_20140729.pdf). These evaluation studies suggest that the assimilation of composition data generally improves the modelled tropospheric ozone fields, noting that there are some exceptions which highlight the fact that assimilation does not always yield a close match with observations and that the results depend on several factors such as the quality and quantity of data being assimilated, and the type of modelling system and the data assimilation methodology used.

The MACC composition reanalysis is given at 60 hybrid sigma-pressure levels, from near the surface (1012 hPa, 10 m Geometric Altitude) to 0.1 hPa (~ 65.6 km) covering both the troposphere and the stratosphere. The global ozone concentration data at the 10-m level were extracted at a horizontal resolution of 1.125° × 1.125° at 3-h time intervals, and were re-gridded to the ACCESS-UKCA N96 horizontal grid using bilinear interpolation. These data were then multiplied by the time-matched 3-h deposition velocity fields obtained from ACCESS-UKCA to obtain deposition flux and total global deposition. The use of a 3-hourly temporal resolution, which is the finest available for the MACC reanalysis, ensures that the diurnal covariance of ozone and deposition velocity is accounted for in calculating total dry deposition. This diurnal covariance for the ocean is likely to be small because the oceanic v_d as parameterised in our model mainly depends on SST which has a relatively weak diurnal dependence (in the model since monthly-averaged SSTs interpolated on daily basis are used there is no diurnal variation of SST anyway) coupled with the fact that ozone concentration in marine air has only a minor diurnal variation (Galbally et al., 2000). However, the diurnal covariance for land surfaces is considerable due to the strong diurnal variations in vertical air exchange in the ABL, in ozone concentrations and in the stomatal uptake which influences v_d. The MACC data for all ten years were used, which is useful for examining interannual variability of deposition.

5.1 Global distribution of surface ozone and dry deposition flux

As an example, Figure 7a shows the mean surface ozone concentration (ppbv) based on the MACC reanalysis for 2005. It is apparent that relatively high concentrations occur in the Northern Hemisphere, particularly in the mid latitudes which can be

attributed to the larger precursor emissions in these areas. The concentrations over the ocean are generally greater than those over the land, which can be partly attributed to the smaller dry deposition velocities to the ocean and hence lower deposition. There are ozone minima around the Equator, especially over the Pacific Ocean.

The annual oceanic ozone dry deposition flux obtained using the MACC ozone reanalysis coupled with the deposition velocities from ACCESS-UKCA averaged over 2005 presented in Figure 7b indicates that the largest flux values between 0.014–0.02 μg m^{-2} s^{-1} are observed within latitudes 10–40°N. The flux in the Southern Hemisphere is lower than that in the Northern Hemisphere and decreases with latitude.

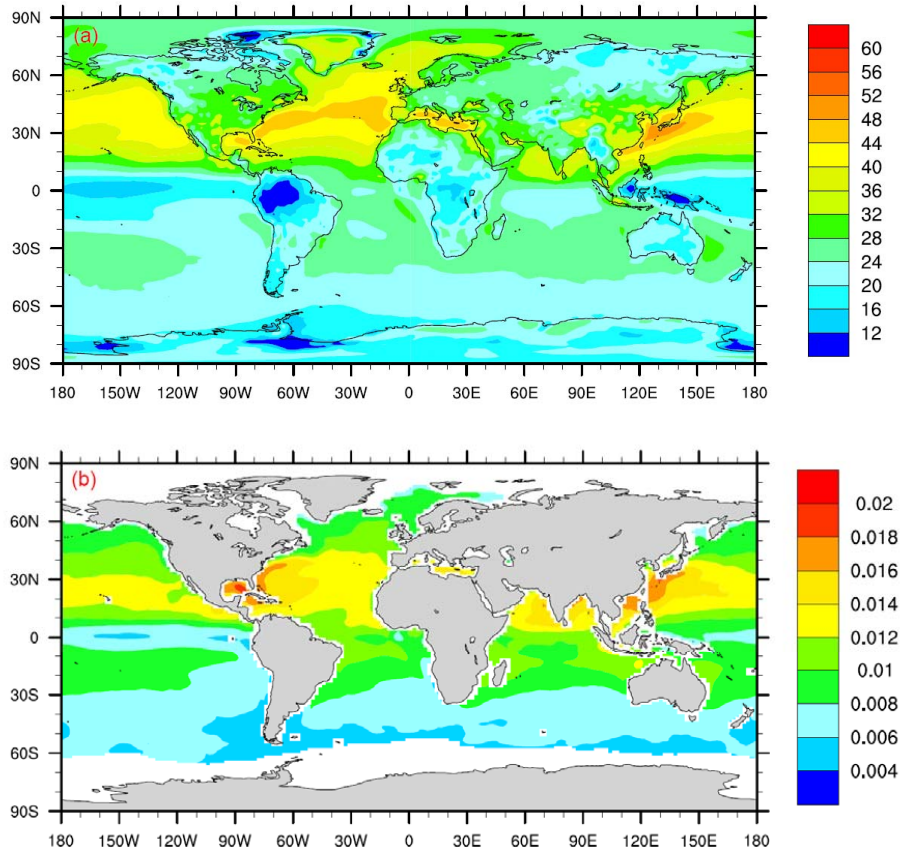

Figure 7: (a) Mean surface ozone concentration (ppbv) and (b) mean oceanic ozone dry deposition flux (μg m^{-2} s^{-1}), for 2005 obtained from the MACC reanalysis.

Atmos. Chem. Phys. Discuss., https://doi.org/10.5194/acp-2017-768
Manuscript under review for journal Atmos. Chem. Phys.
Discussion started: 20 September 2017

Atmospheric Chemistry and Physics Discussions

5.2 Dry deposition budgets

Figure 8 presents the annual ozone dry deposition obtained using the MACC reanalysis as a function of year. The oceanic deposition (Figure 8a) lies between 86.5–108.3 Tg O_3 yr^{-1} with the average being 93.9 ± 7.5 Tg yr^{-1} (see Table 1) where the uncertainty corresponds to one standard deviation and is solely due to interannual variation. The largest deposition occurs for 2005–2007. Oceanic deposition in the Northern Hemisphere (49.0 ± 3.4 Tg yr^{-1}) is somewhat larger than that in the Southern Hemisphere (44.9 ± 4.5 Tg yr^{-1}) due to the higher O_3 concentrations and slightly larger oceanic deposition velocities in the former, although the Earth's area covered by the ocean is larger by approximately 30% in the Southern Hemisphere. There is a hint in Figure 8a that the pattern of interannual variability of the global oceanic deposition follows that for the Southern Hemisphere more closely.

Atmos. Chem. Phys. Discuss., https://doi.org/10.5194/acp-2017-768
Manuscript under review for journal Atmos. Chem. Phys.
Discussion started: 20 September 2017

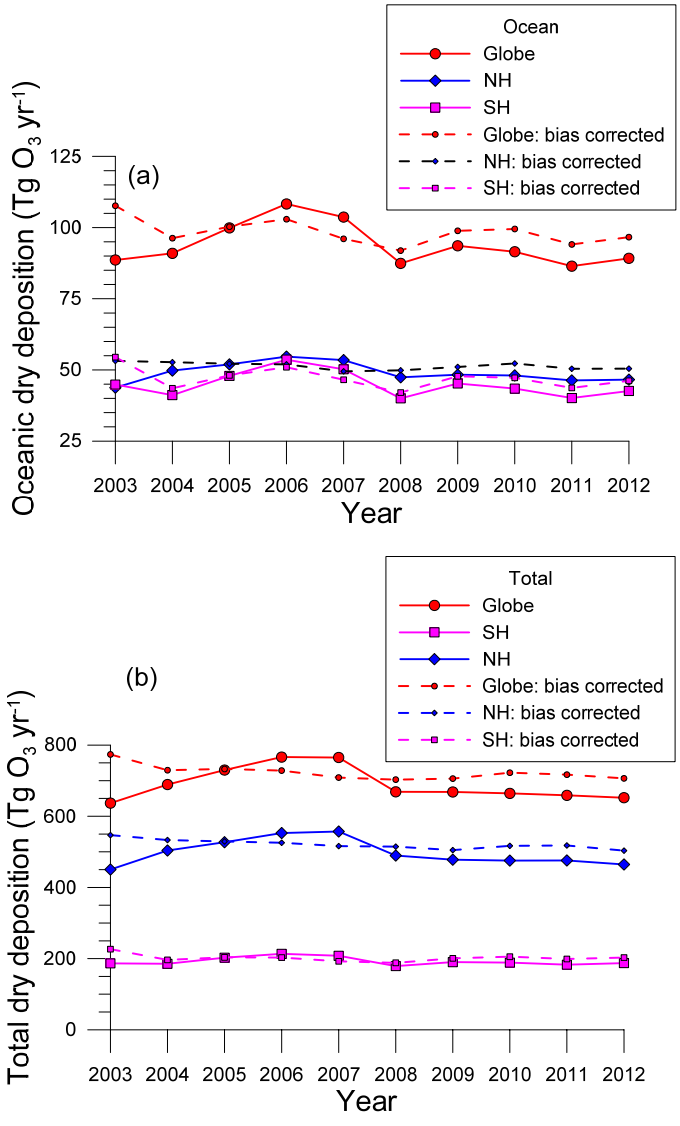

Figure 8: Annual variation of the dry deposition of ozone (Tg O_3 yr^{-1}) obtained using the ACCESS-UKCA model (dotted lines) and the MACC reanalysis (solid lines): (a) the ocean component and (b) total. (NH = Northern Hemisphere, SH = Southern Hemisphere).

The variation of the global total deposition obtained using the MACC reanalysis in Figure 8b is in the range 636.9–766.3 Tg yr^{-1} and the mean value is 689.9 ± 47.0 Tg yr^{-1} (see also Table 1) with the largest deposition amounts for 2005–2007. The total deposition to the Northern Hemisphere (497.5 ± 36.9 Tg yr^{-1}) is 72% of the total deposition and is two and a half times larger than that to the Southern Hemisphere (192.4 ± 11.4 Tg yr^{-1}) because in the former the O_3 concentrations are larger coupled with the larger coverage of the Earth's area by land for which deposition velocities are larger than for water. On average, deposition to the ocean is approximately 14% of the total deposition. The pattern of interannual variability of the global deposition is dominated by that for the Northern Hemisphere. This variability is driven by MACC ozone concentration changes rather than changes in deposition velocity.

The MACC reanalysis is not free from bias as demonstrated in a number of studies (e.g., Inness et al., 2013; Gaudel et al., 2015; Giordano et al., 2015; Katragkou et al., 2015). With regards to global bias in surface ozone, Figure 9 presents the annual averaged normalised median bias (%) of the MACC ozone mixing ratios relative to the Global Atmosphere Watch (GAW) surface observations (http://www.wmo.int/pages/prog/arep/gaw/gaw_home_en.html) for the years 2003–2012. We have derived this bias using the seasonal bias data taken from Benedictow et al. (2014) (http://macc.copernicus-atmosphere.eu/documents/maccii/deliverables/val/MACCII_VAL_DEL_D_83.6_REAreport04_20140729.pdf). Figure 9 shows that except for the first year the bias has remained within ±10%, and has been negative since 2008. The bias is the smallest for the year 2005. The total deposition for that year is 729.8 Tg yr^{-1} of which 527.1 Tg yr^{-1} is to the Northern Hemisphere and 202.7 Tg yr^{-1} is to the Southern Hemisphere. The total oceanic deposition for that year is 99.9 Tg yr^{-1} of which 52.0 Tg yr^{-1} is to the Northern Hemisphere and 47.9 Tg yr^{-1} is to the Southern Hemisphere. Thus the total deposition to non-water surfaces is 629.9 Tg yr^{-1}.

Interestingly, the shape of the interannual variation of total deposition in Figure 8b (and also the interannual variation of total oceanic deposition in Figure 8a) is similar to that of the bias in Figure 9, suggesting that the interannual variability of dry deposition may at least partly be due to the interannual variability of bias in the MACC ozone. Figure 10 is a scatter plot of the annual averaged bias (%) in the MACC ozone versus the total global deposition and total oceanic deposition determined based on the MACC data for the years 2003–2012. The annual bias and deposition appear well correlated, with a liner correlation coefficient of $r^2 = 0.83$ for the total deposition and $r^2 = 0.65$ for the oceanic deposition. Based on the linear fits, the annual ozone deposition value corresponding to zero bias is 717.6 Tg yr^{-1} for the globe and 97.8 Tg yr^{-1} for the ocean.

Atmos. Chem. Phys. Discuss., https://doi.org/10.5194/acp-2017-768
Manuscript under review for journal Atmos. Chem. Phys.
Discussion started: 20 September 2017

Atmospheric Chemistry and Physics Discussions

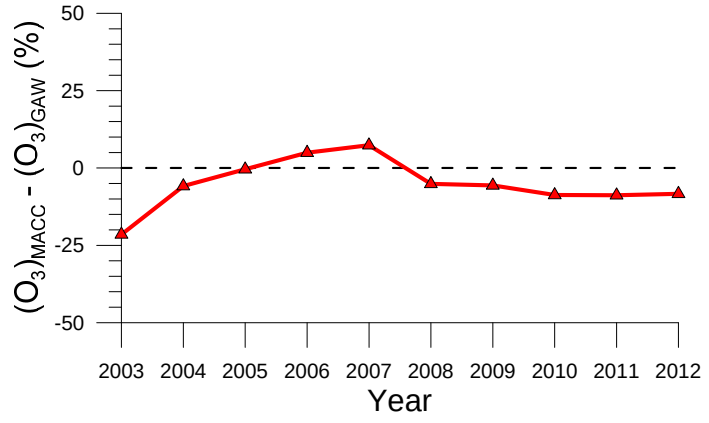

Figure 9: Annual averaged normalised median bias (%) of the MACC ozone reanalysis mixing ratios relative to the Global Atmosphere Watch (GAW) surface observations for the years 2003–2012.

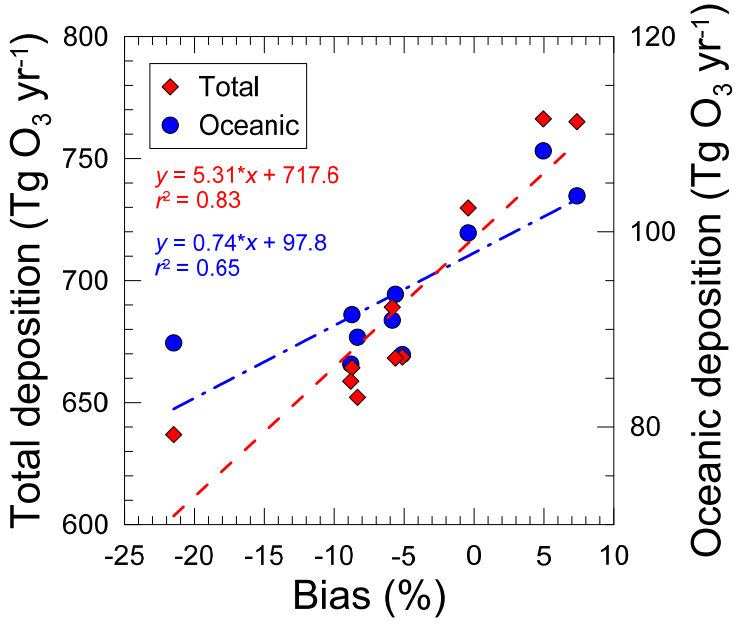

Figure 10: Scatter plot of annual averaged normalised median bias (%) in the MACC ozone reanalysis mixing ratios relative to the Global Atmosphere Watch (GAW) surface observations for the years 2003–2012 versus the total global deposition and total deposition to the ocean determined based on the MACC reanalysis. The best fit lines are also shown.

Atmos. Chem. Phys. Discuss., https://doi.org/10.5194/acp-2017-768
Manuscript under review for journal Atmos. Chem. Phys.
Discussion started: 20 September 2017

Atmospheric Chemistry and Physics Discussions

The above bias correction does not provide information to annual variability without bias. A simple (but rather crude) way to correct the MACC based deposition (d_{p0}) for each year for the bias (b_s) is to calculate a new annual deposition $d_p = d_{p0}(1 - b_s/100)$ and then calculate the average over the ten years and the corresponding standard deviation. By assuming that the observed global bias is uniform over the land, ocean and hemispheric components, averages and standard deviations for these components can also be derived. The bias corrected deposition values are plotted in Figure 8 and presented in Table 1. The average oceanic deposition is 98.4 ± 4.5 Tg yr^{-1} and the average total global deposition is 722.8 ± 20.9 Tg yr^{-1}. The total deposition to non-water surfaces is 624.4 ± 17.4 Tg yr^{-1}. These averages are very similar to those for the year 2005 and those corresponding to the zero bias in Figure 10.

Table 1: Mean ozone dry deposition based on the MACC data for the years 2003–2012 (Tg O_3 yr^{-1})[1], and from other studies that also report the oceanic component.

Method	Ocean			Land			Total		
	NH	SH	Global	NH	SH	Global	NH	SH	Global
Galbally and Roy (1980)[2]	191	300	491	459	141	600	650	441	1091
Ganzeveld et al. (2009)[3]	-	-	291.5	-	-	543.5	-	-	835
Hardacre et al. (2015)[4]	-	-	340	-	-	638	646	332	978 ± 127
MACC	49.0 ± 3.4	44.9 ± 4.5	93.9 ± 7.5	448.5 ± 33.6	147.5 ± 7.2	596.0 ± 40.0	497.5 ± 36.9	192.4 ± 11.4	689.9 ± 47.0
MACC (bias corrected)	51.3 ± 1.3	47.1 ± 3.7	98.4 ± 4.5	469.6 ± 12.3	154.8 ± 7.3	624.4 ± 17.4	520.9 ± 13.2	201.9 ± 10.2	722.8 ± 20.9

[1]The ocean component excludes sea ice and coastal grid cells and on average covers 62.4% of the Earth's surface; [2]In Galbally and Roy (1980), the oceanic component includes ice and there is an uncertainty of ±50% in their estimates; [3]avearge values from two model runs; [4]the oceanic component is based on the average of values from two different land-cover schemes, and the NH and SH components based on Hardacre (2017, personal communication); NH = Northern Hemisphere, SH = Southern Hemisphere.

The above MACC based deposition amounts can be compared with other studies, going as far back as Galbally and Roy (1980) (see Table 1). The total land-based deposition in Galbally and Roy (1980) is similar to the present estimates but their oceanic deposition is five times as large. This may partly be due to the fact that at that time there were only coastal measurements of ozone uptake by seawater with larger deposition velocities than for the open ocean.

More recently, Hardacre et al. (2015) analysed monthly ozone dry deposition fluxes from 15 global chemistry transport models (not including UKCA) driven by meteorological fields for the year 2001. These models use Wesely's scheme (1989) for the deposition velocity calculation for both water and terrestrial surfaces. ACCESS-UKCA also uses Wesely's scheme for terrestrial surfaces. A comparison of observed dry deposition fluxes with those obtained from the above global chemistry transport models for terrestrial surfaces is presented by Hardacre et al. (2015). These authors noted that differences in ozone dry deposition flux to the ocean, driven by small absolute differences in dry deposition velocity but with large areal coverage by the ocean, are the largest contributor to differences in the total global O_3 deposition compared to any other surface type. They determined that the mean total global deposition was 978 ± 127 Tg O_3 yr^{-1} where the range corresponds to one standard deviation. By using two different land-cover schemes for partitioning fluxes, they determined that deposition to the ocean was in the range 250–591 (average 361) Tg yr^{-1} across the model ensemble using one land-cover scheme that had 71.2% of the Earth's surface covered by water, and 209–538 (average 319) Tg yr^{-1} using the other that had 68.6% of the global surface covered by water. The modelling study by Ganzeveld et al. (2009) points to an oceanic dry deposition estimate of 283–300 Tg yr^{-1} and a global total of 833–837 Tg yr^{-1} (Table 1). The oceanic deposition budgets in all these studies are more than three times larger than the 98.4 Tg yr^{-1} value obtained in the present study. This much of difference cannot be explained by the slightly lower fraction of the global surface covered by water in the present calculations (i.e. 62.4%). The primary reason for this difference, as alluded earlier, is that the global chemistry transport models in these studies are all largely based on Wesely's (1989) deposition scheme which uses a constant surface resistance for water. As shown by Luhar et al. (2017) the use of $r_c = 2200$ s m^{-1} overestimates open ocean deposition velocity compared to the open-ocean measurements of Helmig et al. (2012) by a factor of 2 to 4. The smaller oceanic deposition budget presented in this paper is consistent with these currently best available open-ocean measurements. The total deposition to non-water surfaces based on the MACC data is 624.4 Tg yr^{-1}, which is similar to 638 Tg yr^{-1} obtained by Hardacre et al. (2015) (using an average oceanic deposition of 340 Tg yr^{-1} in their calculations) and 600 Tg yr^{-1} obtained by Galbally and Roy (1980).

There are other studies that report on the total global dry deposition. Stevenson et al. (2006) report an average global ozone dry deposition of 1003 ± 200 Tg yr^{-1} for the year 2000 based on 21 models. The average deposition calculated by Wild et al. (2007) using 17 post 2000 modelling studies is 949 ± 222 Tg yr^{-1} whereas that reported by Young et al. (2013) for the year 2000 based on a subset of six models participating in the ACCMIP intercomparison study is 1094 ± 264 Tg yr^{-1}. However, these studies do not report values of the oceanic deposition separately.

It is clear from the above comparison that the land component of the total deposition remains similar in all the studies (after subtracting an oceanic contribution of ~ 300 Tg yr^{-1} from the total in the previous studies). The new estimate of dry deposition to the ocean of ~ 100 Tg O_3 yr^{-1} is approximately a third of the current model estimates. This reduction corresponds to an approximately 67% decrease in the modelled oceanic dry deposition and 20% decrease in the modelled total dry deposition.

Using the tropospheric ozone budgets given in IPCC (2013) based on Young et al. (2013), we estimate that the reduction in the modelled dry deposition rate by ~ 200 Tg O_3 yr^{-1} over the ocean presented here results in roughly 5% increase in modelled tropospheric ozone burden and an equivalent increase in tropospheric ozone lifetime. In the marine boundary layer at mid to high latitudes, the effect of the ozone increase would be expected to be larger.

6 Conclusions

The ocean phase surface resistance term dominates over aerodynamic and atmospheric viscous sublayer resistances in commonly used parameterisations of ozone dry deposition velocity at the oceanic surface. Recent mechanistic schemes used to parameterise the oceanic surface resistance include the simultaneous effects of ozone solubility in water, waterside molecular diffusion and turbulent transfer, and first-order chemical reaction of ozone with dissolved iodide. Luhar et al. (2017) formulated a semi-empirical scheme that described existing deposition velocity data well, but in order to compensate for the impact of overestimation of turbulent transfer within the waterside viscous sublayer it put an artificial limit on the iodide concentration to a fixed depth of the order of a few micrometres from the water surface whereas in reality iodide is present through the depth of the oceanic mixing layer. Here we presented a simple, analytical two-layer formulation for the oceanic surface resistance that avoids making this limiting assumption. Instead, it makes the valid assumption that the influence of turbulent transfer can be neglected compared to the influence of chemical reaction within the top layer of water that is of the order of the reaction-diffusion length scale (typically a few micrometres). In the water layer below, both chemical reaction and turbulent transfer act together and are accounted for. The new scheme has an asymptotic behaviour that is consistent with the current limits of ozone dry deposition when either chemical reaction or turbulent transfer dominate. When compared against the available observed deposition velocity dependencies on sea surface temperature, the performance of the new two-layer dry deposition scheme within the global chemistry-climate model ACCESS-UKCA (at UM vn8.4) was found to be good..

The mean ozone deposition calculated using the new oceanic deposition scheme in ACCESS-UKCA for 2003–2012 is 86.1 ± 0.9 Tg yr^{-1} for the ocean and 566.7 ± 4.9 Tg yr^{-1} for the globe (the oceanic surface excludes sea ice and coastal grid cells and on average covers 62.4% of the Earth's surface). The tendency for ACCESS-UKCA to underestimate observed tropospheric ozone concentrations leads to a lower estimate of the dry deposition flux and hence its budget. By using the 3-h MACC reanalysis for ozone concentration for the years 2003–2012 and the corresponding 3-h deposition velocity values

obtained from ACCESS-UKCA (using the new dry deposition scheme for the ocean presented here and the default scheme for the other surface types), the deposition budget has been recalculated and quantified. The MACC based average global oceanic deposition of ozone is 93.9 ± 7.5 Tg yr^{-1} and the average total global deposition is 689.9 ± 47.0 Tg yr^{-1} with the largest deposition amounts for the years 2005–2007. The interannual variability in deposition is correlated with bias in the MACC ozone mixing rations. When deposition is selected for the minimum bias the annual ozone deposition value is 722.8 ± 20.9 Tg yr^{-1} for the globe and 98.4 ± 4.5 Tg yr^{-1} for the ocean. This new estimate of oceanic dry deposition represents a reduction of approximately 67% over the current estimates of oceanic deposition. This reduction leads to a 20% decrease in the modelled total global dry deposition an increase of approximately 5% in the modelled tropospheric ozone burden and an equivalent increase in tropospheric ozone lifetime.

Acknowledgements

This research was undertaken with the assistance of resources and services from the National Computational Infrastructure (NCI), which is supported by the Australian government. Luke Abraham of University of Cambridge, and Fiona O'Connor and Mohit Dalvi of the U.K. Met Office are thanked for their assistance with the UM-UKCA model. C. Hardacre is acknowledged for providing additional details of their published deposition work. ERA-Interim data from the European Centre for Medium-Range Weather Forecasts and the ozone reanalysis data from the European MACC program were used in this research.

References

Abraham, N. L., Archibald, A. T., Bellouin, N., Boucher, O., Braesicke, P., Bushell, A., Carslaw, K. S., Collins, W., Dalvi, M., Emmerson, K. M., Folberth, G., Haywood, J., Johnson, C., Kipling, Z., Macintyre, H., Mann, G. W., Telford, P. J., Merikanto, J., Morgenstern, O., O'Connor, F., Ordonez, C., Osprey, S., Pringle, K. J., Pyle, J. A., Rae, J. G. L., Reddington, C. L., Savage, D., Spracklen, D., Stier, P., and West, R.: Unified Model Documentation Paper No. 84: United Kingdom Chemistry and Aerosol (UKCA) Technical Description MetUM Version 8.4. UK Met Office, Exeter (UK), pp. 74, 2012.

Carpenter, L. J., MacDonald, S. M., Shaw, M. D., Kumar, R., Saunders, R. W., Parthipan, R., Wilson, J., and Plane, J. M. C.: Atmospheric iodine levels influenced by sea surface emissions of inorganic iodine, Nature Geoscience, 6, 108–111, DOI: 10.1038/NGEO1687, 2013.

Carpenter, L. J. and Nightingale, P. D.: Chemistry and release of gases from the surface ocean, Chemical Reviews, 115, 4015−4034, DOI: 10.1021/cr5007123, 2015.

Chance, R., Baker, A. R., Carpenter, L., and Jickells, T. D.: The distribution of iodide at the sea surface, Environmental Science: Processes & Impacts, 16, 1841–1859, DOI: 10.1039/c4em00139g, 2014.

Dee, D. P., Uppala, S. M., Simmons, A. J., Berrisford, P., Poli, P., Kobayashi, S., Andrae, U., Balmaseda, M. A., Balsamo, G., Bauer, P., Bechtold, P., Beljaars, A. C. M., van de Berg, L., Bidlot, J., Bormann, N., Delsol, C., Dragani, R., Fuentes, M., Geer, A. J., Haimberger, L., Healy, S. B., Hersbach, H., Holm, E. V., Isaksen, L., Kallberg, P., Kohler, M., Matricardi, M., McNally, A. P., Monge-Sanz, B. M., Morcrette, J.-J., Park, B.-K., Peubey, C., de Rosnay, P., Tavolato, C., Thepaut, J.-N., and Vitarta, F.: The ERA-Interim reanalysis: configuration and performance of the data assimilation system, Q. J. Roy. Meteor. Soc., 137, 553–597, doi:10.1002/qj.828, 2011.

Emmons, L. K., Walters, S., Hess, P. G., Lamarque, J.-F., Pfister, G. G., Fillmore, D., Granier, C., Guenther, A., Kinnison, D., Laepple, T., Orlando, J., Tie, X., Tyndall, G., Wiedinmyer, C., Baughcum, S. L., and Kloster, S.: Description and evaluation of the Model for Ozone and Related chemical Tracers, version 4 (MOZART-4), Geosci. Model Dev., 3, 43–67, doi:10.5194/gmd-3-43-2010, 2010.

Fairall, C. W., Hare, J. E., Edson, J. B., and McGillis, W.: Parameterization and micrometeorological measurements of air-sea gas transfer, Bound.-Layer Meteorol., 96, 63–105, DOI: 10.1023/A:1002662826020, 2000.

Fairall, C. W., Hare, J. E., Helmig, D., and Ganzveld, L.: Water-side turbulence enhancement of ozone deposition to the ocean, Atmos. Chem. Phys., 7, 443–451, doi:10.5194/acp-7-443-2007, 2007.

Galbally, I. E. and Roy C. R.: Destruction of ozone at the Earth's surface, Q. J. R. Meteorol. Soc., 106, 599–620, doi:10.1002/qj.49710644915, 1980.

Galbally, I. E., Bentley, S. T., and Meyer, C. P.: Mid-latitude marine boundary-layer ozone destruction at visible sunrise observed at Cape Grim, Tasmania, 41°S, Geophysical Research Letters, 27, 3841–3844, DOI: 10.1029/1999GL010943 2000.

Ganzeveld, L., Helmig, D., Fairall, C., Hare, J. E., and Pozzer, A.: Atmosphere-ocean ozone exchange: A global modeling study of biogeochemical, atmospheric and water-side turbulence dependencies, Global Biogeochem. Cycles, 23, GB4021, doi:10.1029/2008GB003301, 2009.

Garland, J. A., Elzerman, A. W., and Penkett, S. A.: The mechanism for dry deposition of ozone to seawater surfaces, J. Geophys. Res., 85, 7488–7492, doi:10.1029/JC085iC12p07488, 1980.

Gaudel, A., Clark, H., Thouret, V., Jones, L., Inness, A., Flemming, J., Stein, O., Huijnen, V., Eskes, H., Nédélec, P., and Boulanger, D.: On the use of MOZAIC-IAGOS data to assess the ability of the MACC reanalysis to reproduce the distribution of ozone and CO in the UTLS over Europe, Tellus B, 67, 27955, doi:10.3402/tellusb.v67.27955, 2015.

Geernaert, L. L. S., Geernaert, G. L., Granby, K., and Asman, W. A. H.: Fluxes of soluble gases in the marine atmospheric surface layer, Tellus B, 50, 111–127, doi:10.1034/j.1600-0889.1998.t01-1-00001.x, 1998.

Giordano, L., Brunner, D., Flemming, J., Hogrefe, C., Im, U., Bianconi, R., Badia, A., Balzarini, A., Baró, R., Chemel, C., Curci, G., et al.: Assessment of the MACC reanalysis and its influence as chemical boundary conditions for regional air quality modeling in AQMEII-2, Atmospheric Environment, 115, 371–388, doi:10.1016/j.atmosenv.2015.02.034, 2015.

Hardacre, C., Wild, O., and Emberson, L.: An evaluation of ozone dry deposition in global scale chemistry climate models, Atmospheric Chemistry and Physics, 15, 6419–6436, doi:10.5194/acp-15-6419-2015, 2015.

Helmig, D., Lang, E. K., Bariteau, L., Boylan, P., Fairall, C. W., Ganzeveld, L., Hare, J. E., Hueber, J., and Pallandt, M.: Atmosphere-ocean ozone fluxes during the TexAQS 2006, STRATUS 2006, GOMECC 2007, GasEx 2008, and AMMA 2008 cruises, J. Geophys. Res., 117, D04305, doi:10.1029/2011JD015955, 2012.

Hu, J. H., Shi, Q., Davidovits, P., Worsnop, D. R., Zahniser, M. S., and Kolb, C. E.: Reactive uptake of Cl_2(g) and Br_2(g) by aqueous surfaces as a function of Br^- and I^- ion concentration: The effect of chemical reaction at the interface, J. Phys. Chem., 99, 8768–8776, doi:10.1021/j100021a050, 1995.

Inness, A., Baier, F., Benedetti, A., Bouarar, I., Chabrillat, S., Clark, H., Clerbaux, C., Coheur, P., Engelen, R. J., Errera, Q., Flemming, J., George, M., Granier, C., Hadji-Lazaro, J., Huijnen, V., Hurtmans, D., Jones, L., Kaiser, J. W., Kapsomenakis, J., Lefever, K., Leitão, J., Razinger, M., Richter, A., Schultz, M. G., Simmons, A. J., Suttie, M., Stein, O., Thépaut, J.-N., Thouret, V., Vrekoussis, M., Zerefos, C., and the MACC team: The MACC reanalysis: an 8 yr data set of atmospheric composition, Atmos. Chem. Phys., 13, 4073–4109, doi:10.5194/acp-13-4073-2013, 2013.

IPCC: Climate Change 2013: The Physical Science Basis, Contribution of Working Group I to the Fifth Assessment Report of the Intergovernmental Panel on Climate Change, edited by: Stocker, T. F., Qin, D., Plattner, G.-K., Tignor, M., Allen, S. K., Boschung, J., Nauels, A., Xia, Y., Bex, V., and Midgley, P. M., Cambridge University Press, Cambridge, United Kingdom and New York, NY, USA, 1535 pp., 2013.

Johnson, P. N. and Davis, R. A.: Diffusivity of ozone in water, Journal of Chemical & Engineering Data, 41, 1485–1487, DOI: 10.1021/je9602125, 1996.

Katragkou, E., Zanis, P., Tsikerdekis, A., Kapsomenakis, J., Melas, D., Eskes, H., Flemming, J., Huijnen, V., Inness, A., Schultz, M. G., Stein, O., and Zerefos, C. S.: Evaluation of near-surface ozone over Europe from the MACC reanalysis, Geosci. Model Dev., 8, 2299–2314, doi:10.5194/gmd-8-2299-2015, 2015.

Kerkweg, A., Buchholz, J., Ganzeveld, L., Pozzer, A., Tost, H., and Jockel, P., Technical Note: An implementation of the dry removal processes DRY DEPosition and SEDImentation in the Modular Earth Submodel System (MESSy), Atmos. Chem. Phys., 6, 4617–4632, doi:10.5194/acp-6-4617-2006, 2006.

Kinnison, D. E., Brasseur, G. P., Walters, S., Garcia, R. R., Marsh, D. R., Sassi, F., Harvey, V. L., Randall, C. E., Emmons, L., Lamarque, J. F., Hess, P., Orlando, J. J., Tie, X. X., Randel, W., Pan, L. L., Gettelman, A., Granier, C., Diehl, T., Niemeier, U., and Simmons, A. J.: Sensitivity of chemical tracers to meteorological parameters in the MOZART-3 chemical transport model, J. Geophys. Res., 112, D03303, doi:10.1029/2008JD010739, 2007.

Lamarque, J.-F., Emmons, L. K., Hess, P. G., Kinnison, D. E., Tilmes, S., Vitt, F., Heald, C. L., Holland, E. A., Lauritzen, P. H., Neu, J., Orlando, J. J., Rasch, P. J., and Tyndall, G. K.: CAM-chem: description and evaluation of interactive atmospheric chemistry in the Community Earth System Model, Geosci. Model Dev., 5, 369–411, doi:10.5194/gmd-5-369-2012, 2012.

Liu, Q., Schurter, L. M., Muller, C. E., Aloisio, S., Francisco, J. S., and Margerum, D. W.: Kinetics and mechanisms of aqueous ozone reactions with bromide, sulfite, hydrogen sulfite, iodide, and nitrite ions, Inorg. Chem., 40, 4436–4442, doi:10.1021/ic000919j, 2001.

Luhar, A. K., Galbally, I. E., Woodhouse, M. T., and Thatcher, M.: An improved parameterisation of ozone dry deposition to the ocean and its impact in a global climate-chemistry model, Atmos. Chem. Phys., 17, 3749–3767, doi:10.5194/acp-17-3749-2017, 2017.

MacDonald, S. M., Gómez Martín, J. C., Chance, R., Warriner, S., Saiz-Lopez, A., Carpenter, L. J., and Plane, J. M. C.: A laboratory characterisation of inorganic iodine emissions from the sea surface: dependence on oceanic variables and parameterisation for global modelling, Atmos. Chem. Phys., 14, 5841−5852, doi:10.5194/acp-14-5841-2014, 2014.

Magi, L., Schweitzer, F., Pallares, C., Cherif, S., Mirabel, P., and George, C.: Investigation of the uptake rate of ozone and methyl hydroperoxide by water surfaces, J. Phys. Chem. A, 101, 4943–4949, DOI: 10.1021/jp970646m, 1997.

Mao, J., Paulot, F., Jacob, D. J., Cohen, R. C., Crounse, J. D., Wennberg, P. O., Keller, C. A., Hudman, R. C., Barkley, M. P., and Horowitz, L. W.: Ozone and organic nitrates over the eastern United States: Sensitivity to isoprene chemistry, Journal of Geophysical Research: Atmospheres, 118, 11,256-211,268, doi:10.1002/jgrd.50817, 2013.

Monks, P. S., Archibald, A. T., Colette, A., Cooper, O., Coyle, M., Derwent, R., Fowler, D., Granier, C., Law, K. S., Mills, G. E., Stevenson, D. S., Tarasova, O., Thouret, V., von Schneidemesser, E., Sommariva, R., Wild, O., and Williams, M. L.: Tropospheric ozone and its precursors from the urban to the global scale from air quality to short-lived climate forcer, Atmos. Chem. Phys., 15, 8889–8973, doi:10.5194/acp-15-8889-2015, 2015.

Morgenstern, O., Braesicke, P., O'Connor, F. M., Bushell, A. C., Johnson, C. E., Osprey, S. M., and Pyle, J. A.: Evaluation of the new UKCA climate-composition model - Part 1: The stratosphere, Geoscientific Model Development, 2, 43–57, doi:10.5194/gmd-2-43-2009, 2009.

Morris, J.C.: The aqueous solubility of ozone—A review, Ozone news, 1, 14–16, 1988.

O'Connor, F. M., Johnson, C. E., Morgenstern, O., Abraham, N. L., Braesicke, P., Dalvi, M., Folberth, G. A., Sanderson, M. G., Telford, P. J., Voulgarakis, A., Young, P. J., Zeng, G., Collins, W. J., and Pyle, J. A.: Evaluation of the new UKCA climate-composition model - Part 2: The Troposphere, Geoscientific Model Development, 7, 41–91, doi:10.5194/gmd-7-41-2014, 2014.

Soloviev, A. and Lukas, R.: The Near-Surface Layer of the Ocean: Structure, Dynamics and Applications. 2nd ed. Atmospheric and Oceanographic Sciences Library, Vol. 48, Springer, 552 pp., doi 10.1007/978-94-007-7621-0, 2014.

Stevenson, D. S., Dentener, F. J., Schultz, M. G., Ellingsen, K., van Noije, T. P. C., Wild, O., Zeng, G., Amann, M., Atherton, C. S., Bell, N., Bergmann, D. J., Bey, I., Butler, T., Cofala, J., Collins, W. J., Derwent, R. G., Doherty, R. M., Drevet, J., Eskes, H. J., Fiore, A. M., Gauss, M., Hauglustaine, D. A., Horowitz, L. W., Isaksen, I. S. A., Krol, M. C., Lamarque, J.-F., Lawrence, M. G., Montanaro, V., Müller, J.-F., Pitari, G., Prather, M. J., Pyle, J. A., Rast, S., Rodriguez, J. M., Sanderson, M. G., Savage, N. H., Shindell, D. T., Strahan, S. E., Sudo, K., and Szopa, S.: Multimodel ensemble simulations of present-day and near-future tropospheric ozone, Journal of Geophysical Research, 111, D08301, doi:10.1029/2005JD006338, 2006.

Uhe, P. and Thatcher, M.: A spectral nudging method for the ACCESS1.3 atmospheric model, Geoscientific Model Development, 8, 1645–1658, doi:10.5194/gmd-8-1645-2015, 2015.

van der Werf, G. R., Randerson, J. T., Giglio, L., van Leeuwen, T. T., Chen, Y., Rogers, B. M., Mu, M., van Marle, M. J. E., Morton, D. C., Collatz, G. J., Yokelson, R. J., Kasibhatla, P. S.: Global fire emissions estimates during 1997–2015, Earth Syst. Sci. Data Discuss., doi:10.5194/essd-2016-62, 2017

von Kuhlmann, R., Lawrence, M. G., Crutzen, P. J., and Rasch, P. J.: A model for studies of tropospheric ozone and nonmethane hydrocarbons: Model description and ozone results, J. Geophys. Res., 108(D9), 4294, doi:10.1029/2002JD002893, 2003.

Wesely, M.: Parameterization of surface resistances to gaseous dry deposition in regional-scale numerical-models, Atmospheric Environment, 23, 1293–1304, doi:10.1016/0004-6981(89)90153-4, 1989.

Wild, O.: Modelling the global tropospheric ozone budget: Exploring the variability in current models, Atmos. Chem. Phys., 7, 2643–2660, doi:10.5194/acp-7-2643-2007, 2007.

Woodhouse, M. T., Luhar, A. K., Stevens, L., Galbally, I., Thatcher, M., Uhe, P., Wolff, H., Noonan, J., and Molloy, S.: Australian reactive-gas emissions in a global chemistry-climate model and initial results, Air Quality and Climate Change, 49, 31-38, 2015.

Young, P. J., Archibald, A. T., Bowman, K. W., Lamarque, J.-F., Naik, V., Stevenson, D. S., Tilmes, S., Voulgarakis, A., Wild, O., Bergmann, D., Cameron-Smith, P., Cionni, I., Collins, W. J., Dalsøren, S. B., Doherty, R. M., Eyring, V., Faluvegi, G., Horowitz, L. W., Josse, B., Lee, Y. H., MacKenzie, I. A., Nagashima, T., Plummer, D. A., Righi, M., Rumbold, S. T., Skeie, R. B., Shindell, D. T., Strode, S. A., Sudo, K., Szopa, S., and Zeng, G.: Pre-industrial to end 21st century projections of tropospheric ozone from the Atmospheric Chemistry and Climate Model Intercomparison Project (ACCMIP), Atmos. Chem. Phys., 13, 2063–2090, doi:10.5194/acp-13-2063-2013, 2013.